

## New adaptive time step symplectic integrator: an application to the elliptic restricted three-body problem \*

Xiao-Ting Ni and Xin Wu

Department of Physics, Nanchang University, Nanchang 330031, China; [xwu@ncu.edu.cn](mailto:xwu@ncu.edu.cn)

Received 2013 December 19; accepted 2014 March 26

**Abstract** The time-transformed leapfrog scheme of Mikkola & Aarseth was specifically designed for a second-order differential equation with two individually separable forms of positions and velocities. It can have good numerical accuracy for extremely close two-body encounters in gravitating few-body systems with large mass ratios, but the non-time-transformed one does not work well. Following this idea, we develop a new explicit symplectic integrator with an adaptive time step that can be applied to a time-dependent Hamiltonian. Our method relies on a time step function having two distinct but equivalent forms and on the inclusion of two pairs of new canonical conjugate variables in the extended phase space. In addition, the Hamiltonian must be modified to be a new time-transformed Hamiltonian with three integrable parts. When this method is applied to the elliptic restricted three-body problem, its numerical precision is explicitly higher by several orders of magnitude than the nonadaptive one's, and its numerical stability is also better. In particular, it can eliminate the overestimation of Lyapunov exponents and suppress the spurious rapid growth of fast Lyapunov indicators for high-eccentricity orbits of a massless third body. The present technique will be useful for conservative systems including  $N$ -body problems in the Jacobian coordinates in the field of solar system dynamics, and nonconservative systems such as a time-dependent barred galaxy model in a rotating coordinate system.

**Key words:** celestial mechanics — methods: numerical — planetary systems — chaos

### 1 INTRODUCTION

Because of the preservation of geometric structure in a Hamiltonian flow and the absence of secular errors in the integrals of motion, symplectic integrators have become widely popular in long-term integrations of Hamiltonian systems. The obtained desirable properties are generally restricted to the use of a fixed time step. However, the constant time step makes the algorithm have poor performance for the motion of objects in highly eccentric orbits or when close encounters between objects occur. Instead, an adaptive time step that uses a suitable time transformation algorithm rather than coordinate transformations is required<sup>1</sup>. Unfortunately, this leads to the loss of all the benefits of the symplectic method unless a special treatment for the adaptive time step technique is applied.

---

\* Supported by the National Natural Science Foundation of China.

<sup>1</sup> In addition to time transformation, a coordinate transformation such as KS-transformation (Kustaanheimo & Stiefel 1965) is sometimes used.

In practice, the special treatment is the construction of a new time-transformed canonical Hamiltonian to the original system. A symplectic integrator uses a fixed time step for the new Hamiltonian although it is a variable time step algorithm for the original one. So, the symplectic property of the new Hamiltonian flow can be unaffected. Along this idea, many adaptive time step methods have been developed. Mikkola (1997) suggested a few-body problem using a time transformation function, which depends on coordinates and the original physical time. In this sense, the main part containing all the momenta in the time-transformed Hamiltonian is difficult to solve. When it is transformed back to the physical time by using the inversion of the time transformation function, or equivalently the Hamiltonian of Keplerian motion is equipped with a modified mass, it can be solved analytically. Clearly, the practical implementation of such an explicit integrator that uses an adaptive time step is not easy. Preto & Tremaine (1999) gave a suitable choice for the time step function so that the time-transformed Hamiltonian is the sum of two separable integrable parts. As a special case of the proposed step-size selection procedure, the logarithmic Hamiltonian method of Mikkola & Tanikawa (1999) makes the transformation function use two distinct but equivalent forms. This idea was developed by Mikkola & Aarseth (2002). The time transformation is completely adaptive, but not in a Hamiltonian. Emel'yanenko (2007) developed the adaptive time step method further by constructing the time-transformed Hamiltonian. The technique was also applied to study post-Newtonian orbits in a conservative system of stars in the Galactic center (Preto & Saha 2009). In addition, individual symplectic integrators that use a time step for the  $N$ -body Hamiltonian splitting can be seen as a family of adaptive time step methods (Saha & Tremaine 1994; Duncan et al. 1998; Pelupessy et al. 2012). The so-called step size control algorithms should also be adaptive time step methods (Hairer & Söderlind 2005; Seyrich & Lukes-Gerakopoulos 2012). All these adaptive time step symplectic integrators have been shown to be efficient for high-eccentricity orbits whenever close encounters are not of concern.

As a notable problem, although Emel'yanenko refined the time-transformed method of Mikkola & Aarseth, the main Hamiltonian part similar to that of Mikkola (1997) was still not convenient to solve with the analytical method. In view of this, the main aim of this paper is to further develop the time-transformed method of Mikkola & Aarseth. It will be shown in this way that the newly adaptive time step method plays an important role in improving the numerical stability and eliminating the overestimation of chaos indicators involving Lyapunov exponents (Tancredi et al. 2001) and fast Lyapunov indicators (Froeschlé et al. 1997) for high-eccentricity orbits of a massless third body in the elliptic restricted three-body problem (Szebehely 1967).

The paper is organized as follows. We provide a brief review of time-transformed methods and a refinement to the time-transformed method of Mikkola & Aarseth in Section 2. When the newly adaptive time step method is applied to work out the elliptic restricted three-body problem, numerical tests regarding the accuracy of an integral of motion and the reliability of chaos indicators are described in Section 3. Section 4 contains a brief summary.

## 2 TIME-TRANSFORMED METHODS

As claimed in the Introduction, the use of an explicit symplectic integrator with an adaptive time step is indeed based on the construction of a time transformation of the equations of motion or that of a time-transformed Hamiltonian. There have been a number of attempts concerning time transformations; some of them are listed here, and a refinement to the time-transformed method of Mikkola & Aarseth (2002) is given.

### 2.1 Review of Time-transformed Methods

Usually, a time-dependent Hamiltonian is the sum of the kinetic energy  $T$  and the potential energy  $U$  in the separable form

$$H(\mathbf{q}, \mathbf{p}, t) = T(\mathbf{p}) + U(\mathbf{q}, t). \quad (1)$$

Its canonical equations are

$$\begin{aligned} \frac{d\mathbf{q}}{dt} &= \frac{\partial T(\mathbf{p})}{\partial \mathbf{p}}, \\ \frac{d\mathbf{p}}{dt} &= -\frac{\partial U(\mathbf{q}, t)}{\partial \mathbf{q}}. \end{aligned} \tag{2}$$

Taking  $q_0 = t$  as a new coordinate together with the corresponding conjugate momentum  $p_0 = -H$ , one obtains an extended phase space made of variables  $\mathbf{Q} = (q_0, \mathbf{q})$  and  $\mathbf{P} = (p_0, \mathbf{p})$ . Then a modified Hamiltonian is given by

$$\begin{aligned} H^*(\mathbf{Q}, \mathbf{P}) &= T^*(\mathbf{P}) + U(\mathbf{Q}), \\ T^*(\mathbf{P}) &= T(\mathbf{p}) + p_0. \end{aligned} \tag{3}$$

The Hamiltonian is no longer an explicit function of time, so it is a constant, which is zero, the initial value of  $H^*$ . It corresponds to the canonical equations of motion

$$\begin{aligned} \frac{d\mathbf{Q}}{dt} &= \frac{\partial T^*(\mathbf{P})}{\partial \mathbf{P}}, \\ \frac{d\mathbf{P}}{dt} &= -\frac{\partial U(\mathbf{Q})}{\partial \mathbf{Q}}. \end{aligned} \tag{4}$$

Through a time transformation

$$ds = g(\mathbf{Q}, \mathbf{P})dt, \tag{5}$$

Equation (4) can be reexpressed as a generic time-transformed form

$$\begin{aligned} \frac{d\mathbf{Q}}{ds} &= \frac{1}{g(\mathbf{Q}, \mathbf{P})} \frac{\partial T^*(\mathbf{P})}{\partial \mathbf{P}}, \\ \frac{d\mathbf{P}}{ds} &= -\frac{1}{g(\mathbf{Q}, \mathbf{P})} \frac{\partial U(\mathbf{Q})}{\partial \mathbf{Q}}. \end{aligned} \tag{6}$$

The time step function  $g$  is arbitrarily chosen from a mathematical point of view, but not from a physical point of view. Here are two problems. First, Equation (6) is not in the form of canonical equations for a time-transformed Hamiltonian

$$\Gamma(\mathbf{Q}, \mathbf{P}) = \frac{1}{g(\mathbf{Q}, \mathbf{P})} H^*(\mathbf{Q}, \mathbf{P}) \tag{7}$$

unless  $g$  is suitably chosen. Second, both equations in (6) are not individually easily integrable for an arbitrary function  $g$ , even if those equations in Equation (6) are the canonical equations of the Hamiltonian  $\Gamma$ . Thus, the construction of an explicit symplectic integrator fails.

To avoid the two problems, Preto & Tremaine (1999) chose the time step function

$$g(\mathbf{Q}, \mathbf{P}) = \frac{T^*(\mathbf{P}) + U(\mathbf{Q})}{f(T^*(\mathbf{P})) - f(-U(\mathbf{Q}))}, \tag{8}$$

where  $f$  is an arbitrary differentiable function. Substituting (8) in (7), they obtain the Hamiltonian

$$\Gamma(\mathbf{Q}, \mathbf{P}) = f(T^*(\mathbf{P})) - f(-U(\mathbf{Q})). \tag{9}$$

No detailed expression of  $f$  was given, but an explicit symplectic integrator for the Hamiltonian can easily be set up since the two pieces of the Hamiltonian, as separable forms of positions and momenta, are individually easily integrable.

If the function  $f$  is chosen as the natural logarithm, then Equation (9) is a logarithmic Hamiltonian

$$\Gamma(\mathbf{Q}, \mathbf{P}) = \ln(T^*(\mathbf{P})) - \ln(-U(\mathbf{Q})). \tag{10}$$

This is the logarithmic Hamiltonian method of Mikkola & Tanikawa (1999, 2013). In this sense, the Hamiltonian corresponds to the canonical equations

$$\begin{aligned} \frac{d\mathbf{Q}}{ds} &= \frac{1}{T^*(\mathbf{P})} \frac{\partial T^*(\mathbf{P})}{\partial \mathbf{P}}, \\ \frac{d\mathbf{P}}{ds} &= -\frac{1}{-U(\mathbf{Q})} \frac{\partial U(\mathbf{Q})}{\partial \mathbf{Q}}. \end{aligned}$$

That is to say,  $g$  in the upper Equation (6) is  $T^*(\mathbf{P})$ , while in the lower one,  $-U(\mathbf{Q})$ . Note that  $T^*(\mathbf{P}) \equiv -U(\mathbf{Q})$  because  $H^* \equiv 0$  in Equation (3). In other words, the two distinct but equivalent forms are given for the function  $g$ .

In this similar way, Mikkola & Aarseth (2002) introduced a new auxiliary variable

$$W = g(\mathbf{q}(t)), \tag{11}$$

where  $g$  is a function of  $\mathbf{q}$  depending on  $t$ , i.e., an implicit function of  $t$ . In this sense, derivative relations are as follows:  $dt/ds = 1/W = 1/g$ ,  $d\mathbf{q}/ds = (d\mathbf{q}/dt) \cdot dt/ds = (d\mathbf{q}/dt)/W$ ,  $d\mathbf{p}/ds = (d\mathbf{p}/dt) \cdot dt/ds = (d\mathbf{p}/dt)/g$  and  $dW/ds = (dW/dt) \cdot dt/ds = (dg/dt)/g = (\partial g/\partial \mathbf{q} \cdot d\mathbf{q}/dt)/g$ . The time-transformed equations of motion with respect to Equation (2) are

$$\begin{pmatrix} \frac{d\mathbf{q}}{ds} \\ \frac{dt}{ds} \\ \frac{d\mathbf{p}}{ds} \\ \frac{dW}{ds} \end{pmatrix} = \underbrace{\begin{pmatrix} \frac{1}{W} \frac{\partial T}{\partial \mathbf{p}} \\ 1/W \\ 0 \\ 0 \end{pmatrix}}_{\mathbf{A}} + \underbrace{\begin{pmatrix} 0 \\ 0 \\ -\frac{1}{g} \frac{\partial U}{\partial \mathbf{q}} \\ \frac{1}{g} \left( \frac{\partial g}{\partial \mathbf{q}} \cdot \frac{\partial T}{\partial \mathbf{p}} \right) \end{pmatrix}}_{\mathbf{B}}, \tag{12}$$

where both  $\mathbf{A}$  and  $\mathbf{B}$  are individually easily integrable. A composition of the solutions of the two parts, e.g., a leapfrog-like algorithm  $A(\frac{h}{2})B(h)A(\frac{h}{2})$  with  $h$  as a time step, gives an approximate solution to the system (1).

Although an explicit composition algorithm can be derived in terms of Equation (12), it is not symplectic because this equation does not correspond to the canonical equations of a certain time-transformed Hamiltonian. It should be pointed out that the time-transformed method of Mikkola & Aarseth was initially based on equations of motion rather than on a Hamiltonian. In this case, no extended phase space was used. This is why the time-transformed Equation (12) is related to the canonical Equation (2) of the Hamiltonian (1) rather than the canonical Equations (4) of the Hamiltonian (3). Next, we shall supply a time-transformed canonical Hamiltonian by slightly refining the time-transformed method.

### 2.2 A New Time-transformed Method

The Hamiltonian (1) is assumed to have another separable form

$$H(\mathbf{q}, \mathbf{p}, t) = H_0(\mathbf{q}, \mathbf{p}) + H_1(\mathbf{q}, t), \tag{13}$$

where  $H_0$  and  $H_1$  are two integrable Hamiltonians. In the extended phase space, it becomes

$$\begin{aligned} H^*(\mathbf{Q}, \mathbf{P}) &= H_0^*(\mathbf{q}, \mathbf{P}) + H_1(\mathbf{Q}), \\ H_0^*(\mathbf{q}, \mathbf{P}) &= H_0(\mathbf{q}, \mathbf{p}) + p_0. \end{aligned} \tag{14}$$

As in Equation (3),  $H^*$  in Equation (14) is equal to zero. The equations of motion with respect to a first new auxiliary time variable  $\tau$  are rewritten as

$$\begin{aligned} \frac{d\mathbf{q}}{d\tau} &= \frac{\partial H_0(\mathbf{q}, \mathbf{p})}{\partial \mathbf{p}}, \\ \frac{dq_0}{d\tau} &= \frac{\partial H_0^*}{\partial p_0} = 1, \\ \frac{d\mathbf{p}}{d\tau} &= -\frac{\partial H_0(\mathbf{q}, \mathbf{p})}{\partial \mathbf{q}} - \frac{\partial H_1(\mathbf{q}, q_0)}{\partial \mathbf{q}}, \\ \frac{dp_0}{d\tau} &= -\frac{\partial H_1(\mathbf{q}, q_0)}{\partial q_0}. \end{aligned} \tag{15}$$

Setting a second new auxiliary time variable  $s$  with a time transformation

$$\frac{d\tau}{ds} = \frac{1}{W} = \frac{1}{g(\tau)}, \tag{16}$$

$$g(\tau) = g(\mathbf{Q}(\tau), \mathbf{P}(\tau)), \tag{17}$$

where  $g$  is an implicit function of  $\tau$ , we have time-transformed equations

$$\begin{aligned} \frac{d\mathbf{q}}{ds} &= \frac{1}{W} \frac{\partial H_0}{\partial \mathbf{p}}, \\ \frac{dq_0}{ds} &= \frac{1}{W}, \\ \frac{d\mathbf{p}}{ds} &= -\frac{1}{W} \left( \frac{\partial H_0}{\partial \mathbf{q}} + \frac{\partial H_1}{\partial \mathbf{q}} \right) \\ \frac{dp_0}{ds} &= -\frac{1}{W} \frac{\partial H_1}{\partial q_0}, \\ \frac{dW}{ds} &= \frac{\wp}{g}, \\ \wp &= \left[ \frac{\partial g}{\partial \mathbf{q}} \cdot \frac{\partial H_0}{\partial \mathbf{p}} + \frac{\partial g}{\partial q_0} - \frac{\partial g}{\partial \mathbf{p}} \cdot \left( \frac{\partial H_0}{\partial \mathbf{q}} + \frac{\partial H_1}{\partial \mathbf{q}} \right) - \frac{\partial g}{\partial p_0} \cdot \frac{\partial H_1}{\partial q_0} \right]. \end{aligned} \tag{18}$$

Unlike Equation (12), the above equations can be split into three integrable pieces

$$\begin{pmatrix} \frac{d\mathbf{q}}{ds} \\ \frac{dq_0}{ds} \\ \frac{d\tau}{ds} \\ \frac{d\mathbf{p}}{ds} \\ \frac{dp_0}{ds} \\ \frac{dW}{ds} \end{pmatrix} = \begin{pmatrix} \mathbf{A} \\ \mathbf{B} \\ \mathbf{C} \end{pmatrix} = \begin{pmatrix} \frac{1}{W} \frac{\partial H_0}{\partial \mathbf{p}} \\ 1/W \\ \frac{1}{W} - \frac{H_0 + p_0}{W^2} \\ -\frac{1}{W} \frac{\partial H_0}{\partial \mathbf{q}} \\ 0 \\ 0 \end{pmatrix} + \begin{pmatrix} 0 \\ 0 \\ -\frac{H_1}{W^2} \\ -\frac{1}{W} \frac{\partial H_1}{\partial \mathbf{q}} \\ -\frac{1}{W} \frac{\partial H_1}{\partial q_0} \\ 0 \end{pmatrix} + \begin{pmatrix} 0 \\ 0 \\ 0 \\ 0 \\ 0 \\ \frac{\wp}{g} \end{pmatrix}. \tag{19}$$

They are the canonical equations of the time-transformed Hamiltonian

$$\Gamma(\mathbf{q}, q_0, \tau; \mathbf{p}, p_0, W) = \frac{H^*}{W} + \ln \frac{W}{g} = H_A + H_B + H_C, \tag{20}$$

where three sub-Hamiltonians are

$$H_A = \frac{1}{W}(H_0(\mathbf{q}, \mathbf{p}) + p_0) + \ln W, \quad (21)$$

$$H_B = \frac{1}{W}H_1(\mathbf{q}, q_0), \quad (22)$$

$$H_C = -\ln g(\mathbf{q}, q_0, \mathbf{p}, p_0). \quad (23)$$

Two points are worth noting. (i) Since the function  $g$  is considered to be an implicit function of  $\tau$ , perhaps someone casts doubt on how convincing the canonicity of Equation (19) is. Naturally, the terms in Equation (19) represent the canonical equation of the Hamiltonian (20) without any question if the part  $H_C$  (or  $g$ ) is an explicit function of  $\tau$ . However, the result is still true when  $g$  is an implicit function of  $\tau$ . Note that the treatments of the variables  $\mathbf{q}$ ,  $\mathbf{p}$ ,  $q_0$  and  $p_0$  of  $g$  and those in the parts  $H_A$  and  $H_B$  are different. For the former case, they are directly viewed as functions of  $\tau$  so that the canonical equations derived from the Hamiltonian part  $H_C$  are not derivatives with respect to the momenta or the coordinates but are a total derivative of  $g$  with respect to  $\tau$ , not a partial one. For the latter case, they are not directly regarded as functions of time so that the canonical equations derived from the Hamiltonian parts  $H_A$  and  $H_B$  are derivatives with respect to the momenta or coordinates. In this way, Equation (19) can still be the canonical equations of the Hamiltonian (20). In fact, Mikkola & Aarseth (2002), Emel'Yanenko (2007) and Preto & Saha (2009) completely adopted this operation. A similar treatment was made in Galaviz & Brügmann (2011). (ii) Because the Hamiltonian (20) does not explicitly depend on time  $s$ , it should be identical to a constant. Noting that  $\ln(W/g) = 0$  and the starting value of  $H^*$  is zero, we have  $H^* \equiv \Gamma = 0$  for any time  $s$ . This makes it clear that Equation (16) and the equation concerning  $d\tau/ds$  in Equation (19) should be the same although their expressional forms are different.

Obviously, one typical difference between Equations (19) and (12) is that Equation (19) uses the extended phase space in which  $(q_0, p_0)$  is a pair of canonically conjugate variables, and so is  $(\tau, W)$ . If  $\tau$  and  $q_0$  have the same initial values, then  $\tau \equiv q_0$  for any time  $s$ ; when they have different initial values,  $\tau \neq q_0$  can be permitted although  $dt/d\tau = 1$ . However,  $q_0$  and  $\tau$  play different roles in constructing the canonically conjugate variables. This is why we use two time transformations rather than a direct transformation from  $t$  to  $s$ . In this case, there are two canonical extensions from  $H$  to  $\Gamma$ . At first, Equation (14) is used to implement the canonical extension from the  $2n$  dimensional  $H$  to the  $2(n+1)$  dimensional  $H^*$ <sup>2</sup>, and also Equation (20), from the  $H^*$  to the  $2(n+2)$  dimensional  $\Gamma$ <sup>3</sup>. Another important difference lies in that  $g$  appears in the equation with respect to  $\mathbf{p}$  for the Mikkola-Aarseth method, but  $W$  replaces  $g$  for the present method. Notice that  $W$  and  $g$  are exactly equivalent from an analytical point of view but not in the discrete algorithms. There is no explicit conflict between the analysis and the computation. On one hand, the exact equivalence is only required at the initial time and in the derivation of the Hamiltonian (20) from Equations (15)–(19). On the other hand,  $W$  and  $g$  are independently calculated and are not necessarily required to be equivalent in the computation. Besides the two differences between our new method and the method of Mikkola & Aarseth (2002), those between the new method and the method of Emel'Yanenko (2007) are also present. Our  $\tau$  and  $q_0$  are equal for any time  $s$  when the initial values of  $\tau$  and  $q_0$  are 0, but those used in the latter method were not because  $dt = |\mathbf{q}|d\tau$ . As a more explicit difference, our  $\tau$  and  $s$  satisfy the relation (16), but those used in the latter method satisfies the relation  $d\tau = |\mathbf{q}|ds/W$ , which causes it to not be convenient for analytically solving the Hamiltonian part  $H_A$  in Equation (21). Our

<sup>2</sup> This is really the customary canonical extension in classical mechanics. In the extended phase space, the new coordinate  $q_0$  ( $= t$ ) and its canonical momentum  $p_0$  are added. Although the time variable is still  $t$ , we use  $\tau$  as the time variable so as not to confuse  $q_0$  with  $t$ .

<sup>3</sup> In the second canonical extension,  $(\tau, W)$  can be regarded as the canonical conjugate variables which are different from  $(q_0, p_0)$ . For a similar reference, see the method of Emel'Yanenko (2007).

method should certainly contain the method of Preto & Saha (2009) in which only the computation of a conservative Hamiltonian system was discussed.

The new method is very efficient to design explicit symplectic integrators. For example, a second order leapfrog symplectic integrator, as the simplest example of a symmetric symplectic integrator, is

$$S_2(h) = \bar{C}\left(\frac{h}{2}\right)\bar{B}\left(\frac{h}{2}\right)\bar{A}(h)\bar{B}\left(\frac{h}{2}\right)\bar{C}\left(\frac{h}{2}\right), \tag{24}$$

where  $\bar{A}$ ,  $\bar{B}$  and  $\bar{C}$  are Lie derivatives with respect to  $H_A$ ,  $H_B$  and  $H_C$ , respectively. By using a triple product of  $S_2$ , we have the fourth order symplectic integrator of Yoshida (1990)

$$S_4(h) = S_2(\kappa h)S_2(\chi h)S_2(\kappa h) \tag{25}$$

with  $\chi = 1 - 2\kappa$  and  $\kappa = 1/(2 - 2^{1/3})$ . The fourth order algorithm of Forest & Ruth (1990) reads

$$FR = \bar{A}\left(\frac{\kappa}{2}\tau\right)D(\kappa h)\bar{A}\left(\frac{1-\kappa}{2}h\right)D(\chi h)A\left(\frac{1-\kappa}{2}h\right)D(\kappa h)\bar{A}\left(\frac{\kappa}{2}h\right), \tag{26}$$

where  $D$  is a second order approximation

$$D(h) = \bar{C}\left(\frac{h}{2}\right)\bar{B}(h)\bar{C}\left(\frac{h}{2}\right). \tag{27}$$

However, another Forest-Ruth algorithm

$$FR^\dagger = D\left(\frac{\kappa}{2}\tau\right)\bar{A}(\kappa h)D\left(\frac{1-\kappa}{2}h\right)\bar{A}(\chi h)D\left(\frac{1-\kappa}{2}h\right)\bar{A}(\kappa h)D\left(\frac{\kappa}{2}h\right) \tag{28}$$

is only second order because of the non-vanishing third order errors of the operator  $D$ , as was recently confirmed by Mei et al. (2013b). As seen from the original time  $t$ , these symplectic integrators are utilized to adopt adaptive variable time steps.

It is clear that the time-transformed method of Preto & Tremaine (1999), the logarithmic Hamiltonian method of Mikkola & Tanikawa (1999) and the time-transformed method of Mikkola & Aarseth (2002) are not suitable for the Hamiltonian splitting (13) but rather for the Hamiltonian decomposition (1). They become useless for the Hamiltonian splitting of  $N$ -body planetary dynamics in Jacobi coordinates (Wisdom & Holman 1991) or the heliocentric coordinates (Duncan et al. 1998), either. In particular, they fail to work for the circular/elliptic restricted three-body problem (Szebehely 1967) in a rotating coordinate system because its Hamiltonian does not have separable forms of positions and momenta. Similarly, the method of Emel'Yanenko (2007) does not obtain the analytical solution of the Hamiltonian part  $H_A$  of Equation (21) in this case because of the time function  $d\tau = |q|ds/W$ . However, the present method is always efficient for all the cases. Therefore, we only focus on application of the Yoshida construction  $S_4$  to the elliptic restricted three-body problem in the following.

### 3 NUMERICAL COMPARISONS

Suppose that each of two primary objects with masses  $1 - \mu$  and  $\mu$  moves along an elliptic orbit whose eccentricity is  $e_P$  and whose semimajor axis is scaled to unity. In the barycentric rotating coordinate system, the positions of the primaries,  $O_1(\mu, 0)$  and  $O_2(-1 + \mu, 0)$ , are fixed on the  $X$ -axis. Under the gravities of the two bodies, a third massless object (i.e., a test particle) has state variables  $\mathbf{q} = (X, Y)$  and  $\mathbf{p} = (P_X, P_Y)$ , whose evolutions can be determined by the dimensionless Hamiltonian (Szebehely 1967)

$$H = \frac{1}{2}(P_X^2 + P_Y^2) + YP_X - XP_Y - U, \tag{29}$$

where the potential is (Szebehely 1967)

$$U(X, Y, f) = \frac{1}{2} \left( \frac{1}{1 + e_P \cos f} - 1 \right) (X^2 + Y^2) + \frac{1}{1 + e_P \cos f} \left( \frac{1 - \mu}{R_1} + \frac{\mu}{R_2} \right), \quad (30)$$

$$R_1 = [(X - \mu)^2 + Y^2]^{1/2}, \quad (31)$$

$$R_2 = [(X + 1 - \mu)^2 + Y^2]^{1/2}. \quad (32)$$

Note that the true anomaly  $f$ , as the angular position of the main body measured from the pericenter, plays the role of the time variable. This is a dynamical model of the elliptic restricted three-body problem (Szebehely 1967).

According to the description of Section 2.2, we take  $H_0 = (P_X^2 + P_Y^2)/2 + YP_X - XP_Y$  and  $H_1 = -U(X, Y, f)$ . When  $p_0 = -H$  and  $q_0 = f$  are included in the extended phase space, we have the Hamiltonian  $H^* = H_0^* + H_1$  with  $H_0^* = H_0 + p_0$ . Given the time step function

$$g = 1 + c_1 R_1 + c_2 R_2 + \frac{c_3}{R_1} + \frac{c_4}{R_2} \quad (33)$$

with  $c_1 = c_2 = 10$  and  $c_3 = c_4 = 5$ , the time transformed Hamiltonian  $\Gamma$  (20) with the three separable parts (21)–(23) can be obtained. Note that the function  $g$  chosen as the form (33) is based on the use of smaller time steps when close encounters between the third body and the primary body 1 (or 2) occur, and the values of the parameters  $c_1$ ,  $c_2$ ,  $c_3$  and  $c_4$  are from those which are found to provide the best accuracy in many numerical tests. Next, we shall evaluate the numerical performance of the symplectic integrator  $S_4$  with adaptive time steps.

### 3.1 Accuracy Evaluation

Numerical simulations are implemented according to different values of  $e_P$ .

#### 3.1.1 $e_P = 0$

For the special case  $e_P = 0$ , the Hamiltonian  $H$  is just that of the circular restricted three-body problem (Huang & Wu 2014a). It is conservative because it can be expressed in the Jacobi constant  $C_J$  as

$$H \equiv -\frac{1}{2}C_J, \quad (34)$$

$$C_J \equiv 2U + X^2 + Y^2 - (\dot{X}^2 + \dot{Y}^2). \quad (35)$$

Here, the time variable is the physical time  $t$ .

Let us take the parameters  $C_J = 3.06$  and  $\mu = 0.001$ <sup>4</sup>. The initial conditions are  $Y = \dot{X} = 0$ . The initial value of  $X$  is one of the three values, 0.08, 0.29 and 0.48, which correspond to orbits 1, 2 and 3 respectively. As to the initial value of  $\dot{Y}$ , it is solved from Equation (35). The fixed time step is  $h = 0.01$ . When the algorithm  $S_4$  is applied to integrate the extended phase-space Hamiltonian  $H^*$  in the old time  $t$  or  $\tau$ , we can obtain the state variables  $(X, Y, P_X, P_Y)$  or  $(X, Y, \dot{X}, \dot{Y})$ . In this way, the phase portraits of the three orbits on the Poincaré section  $Y = 0$  with  $\dot{Y} > 0$  can be plotted in Figure 1. This figure makes it clear that orbits 1 and 2 are regular, but orbit 3 is chaotic. In spite of this, the Jacobi constant error for orbits 1 or 2 is much larger than for orbit 3, as shown in Figure 2. This is due to these orbits for the third body having distinct eccentricities,  $e_1 = 0.81$ ,  $e_2 = 0.49$  and  $e_3 = 0.28$ . In general, the larger eccentricity an orbit has, the poorer the accuracy of an integrator becomes.

<sup>4</sup> The value 3.06 for  $C_J$  is one of the values which admit the onset of chaos. The value 0.001 for  $\mu$  is approximately the ratio of Jupiter to the Sun.

When we apply the algorithm  $S_4$  to act on the three orbits in the Hamiltonian  $\Gamma$  in the new time  $s$ , namely the adaptive time step method is used, we have the Jacobi constant errors, labeled as A1, A2 and A3 in Figure 2. Compared with the original nonadaptive time step method, the adaptive one improves the numerical accuracy of the Jacobi constant for each orbit by about 7 orders of magnitude. This shows that the adaptive time step method can give the integrator good numerical performance. What about for the case of  $e_P \neq 0$ ? This will be addressed in the following demonstration.

### 3.1.2 $e_P \neq 0$

If  $e_P \neq 0$ , then the Hamiltonian of the elliptic problem is a periodic function of the true anomaly  $f$ . Here,  $f$  is referred to as a time variable. This tells us that the elliptic problem is a non-autonomous dynamical system. In this case, it no longer possesses an energy integral or the Jacobi constant. In spite of this, the extended Hamiltonian  $H^*$  similar to Equation (14) is always identical to zero for the use of nonadaptive time step methods, as is the extended Hamiltonian  $H^*$  like that of Equation (20) for the use of adaptive time step methods, which is illustrated in point (ii) below Equation (23). Therefore, the Hamiltonian being equal to zero will be used to measure the quality of the numerical methods.

As the eccentricity of the orbit of the primary bodies becomes slightly larger than 0, e.g.  $e_P = 0.005$ , the dynamical structures of the three orbits may be different. This can be clearly seen by comparing Figure 3(a) and Figure 1. An explicit difference lies in that orbit 2 is a quasi-periodic orbit with five islands for  $e_P = 0$ , but it seems to become chaotic for  $e_P = 0.005$ . Of course, the phase portraits of orbits 1 and 3 in the elliptic case have some differences, compared with those in the circular case. However, the accuracy of the extended Hamiltonian  $H^*$  in Figure 3(b) is almost consistent with that of the Jacobi constant in the circular case when the adaptive time step method acts on each orbit. Given  $e_P = 0.01$  or  $e_P = 0.015$ , the adaptive time step method can still give a similar precision to the extended Hamiltonian. In spite of this, the dynamical structures are typically different, as shown in Figure 4. It should be pointed out that when the eccentricity of the orbit of the primary bodies is further increased, the three orbits become unbounded.

It is worth emphasizing that the method of the Poincaré section is very suitable for the description of the dynamical structure of a conservative system whose phase space has four dimensions. For the nonconservative elliptic problem  $H$  whose corresponding conservative extended Hamiltonian  $H^*$  has six dimensions in phase space, the use of the section method in finding chaos would be problematic. It is necessary to employ other methods/indicators such as Lyapunov exponents to study the dynamics of these orbits. On the other hand, it is desired to understand whether the adaptive time step method can ensure the reliability of the indicators.

## 3.2 Chaos Indicators

Unlike the method that plots a Poincaré section, Lyapunov exponents or fast Lyapunov indicators (Froeschlé et al. 1997), as one of the most common qualitative tools for distinguishing chaos from order, is efficient for describing the dynamics of a phase space with any dimension.

### 3.2.1 Lyapunov exponents

The principal Lyapunov exponent is an important indicator for characterizing the average exponential deviation of two nearby orbits. The variational method and the two-particle one are two algorithms for computing the Lyapunov exponent (Tancredi et al. 2001). If an initial separation and the number of renormalizations are suitably considered, the two techniques are confirmed to be effective in detecting the long-term dynamical behavior of orbits. For convenience of application, the former method is often replaced with the latter one in some complicated dynamical systems. As another

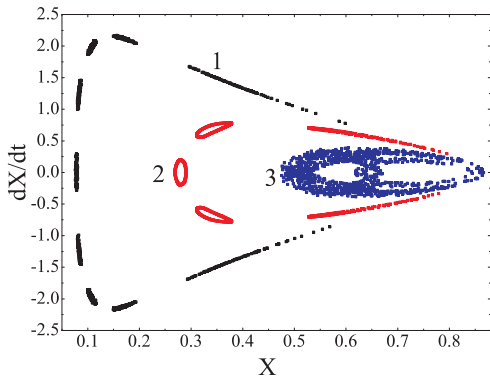


**Fig. 1** Phase portraits of three orbits on the Poincaré section  $Y = 0$  with  $\dot{Y} > 0$  for the circular restricted three-body problem with the eccentricity of the orbit of the primary bodies,  $e_P = 0$ . The three orbits of the third body correspond to the Jacobi constant  $C_J = 3.06$  and eccentricities,  $e_1 = 0.81$ ,  $e_2 = 0.49$  and  $e_3 = 0.28$ .

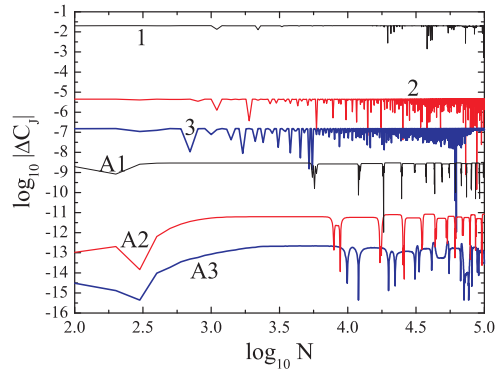


**Fig. 2** Jacobi constant errors of the three orbits in Fig. 1 when the Yoshida construction  $S_4$  and the corresponding adaptive time step methods, A1, A2 and A3, are respectively used. To illustrate this point,  $N$  is the step number of numerical integration.

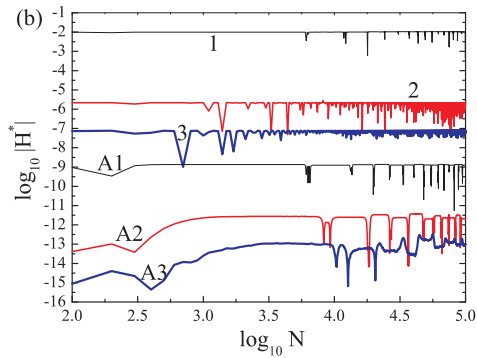
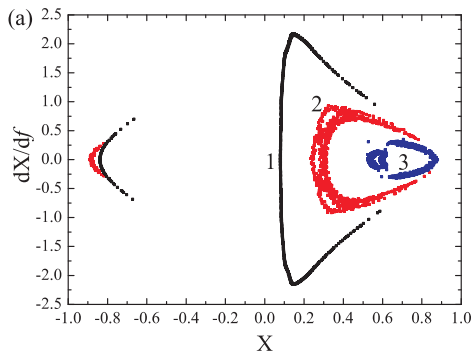


**Fig. 3** Panel (a): the same as Fig. 1 but for the elliptic restricted three-body problem with the eccentricity of the orbit of the primary bodies,  $e_P = 0.005$ . These phase portraits are obtained from the nonadaptive time step methods. Panel (b): accuracy estimation of the extended Hamiltonian  $H^*$  when the nonadaptive and adaptive time step methods are used independently.

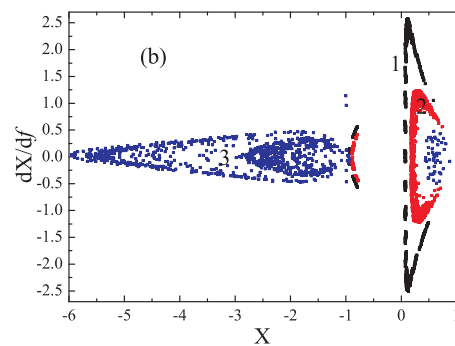
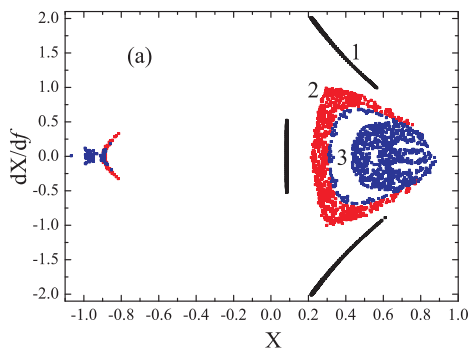


**Fig. 4** The same as Fig. 3(a) but the eccentricities of the central bodies are  $e_P = 0.01$  in panel (a) and  $e_P = 0.015$  in panel (b). Adaptive time step methods are used independently.

advantage for the use of the latter method in the present paper, the symplectic integrators can be used during the whole course of calculation of Lyapunov exponents. This should be viewed as the application of the global symplectic integrators<sup>5</sup> in chaos determination.

The largest Lyapunov exponent with the two-particle method is defined as (Wu & Huang 2003)

$$\lambda = \lim_{t \rightarrow \infty} \frac{1}{t} \log \frac{d(t)}{d(0)}, \tag{36}$$

where the distance between two nearby trajectories at time  $t$  is

$$d(t) = \left[ (X_2 - X_1)^2 + (Y_2 - Y_1)^2 + (P_{X2} - P_{X1})^2 + (P_{Y2} - P_{Y1})^2 \right]^{1/2}. \tag{37}$$

The best choice of the starting separation  $d(0)$  is about an order of  $10^{-8}$  in the double precision of the machine (Tancredi et al. 2001), and the renormalization should be done through 10 steps in the phase space defined by  $(X, Y, q_0, \tau; P_X, P_Y, p_0, W)$ . A bounded orbit is said to be chaotic if  $\lambda > 0$ , but regular when  $\lambda = 0$ .

Panels (a)–(c) in Figure 5 are related to Lyapunov exponents of the three orbits from Figure 1 when the nonadaptive and adaptive time step methods are used independently. To our surprise, the nonadaptive time step method gives a positive Lyapunov exponent to orbit 1, i.e. identifying chaoticity in orbit 1. This result explicitly conflicts with the quasi-periodicity of orbit 1 in Figure 1. The overestimation of the Lyapunov exponent is due to the high orbital eccentricity causing the poorest numerical accuracy in about the order  $10^{-2}$ , as shown in Figure 2. Notice that the error is dramatically larger than the initial distance of the two nearby orbits,  $10^{-8}$ . When the adaptive time step method improves the accuracy in about the order  $10^{-9}$ , the Lyapunov exponent will tend to zero so that correct information about the orbit can be obtained.

Another reason seems to be in numerical instability for the nonadaptive time step method but to maintain good numerical stability for the adaptive one. For orbit 2, the nonadaptive and adaptive time step methods force the Lyapunov exponent to tend to zero, as coincides with the behavior of the orbit in Figure 1. As far as orbit 3 is concerned, the Lyapunov exponent seems to be closer to a stabilizing positive value for the adaptive time step method than for the nonadaptive one. As a result, in contrast to the nonadaptive time step method, the adaptive one not only avoids the overestimation of Lyapunov exponents but also obtains reliable Lyapunov exponents for the circular problem. This result is also correct for the elliptic case with  $e_P = 0.01$  in panels (d)–(f).

As a point to note, the Lyapunov exponents in Figure 5(c), (e) and (f) do not seem to completely reach stabilizing positive values even if the adaptive time step method is taken into account. This shows that computation of such stabilizing values is too expensive. Instead, fast Lyapunov indicators are quicker and more sensitive methods to identify chaos. In the following, let us focus on how the adaptive time step method exerts influence on them.

### 3.2.2 Fast Lyapunov indicators

The length of a tangential vector from the variational equations increases in completely different time rates for ordered and chaotic orbits. On the basis of this, Froeschlé et al. (1997) proposed three fast Lyapunov indicators (FLIs) to distinguish between the two cases. Then the natural logarithm of the magnitude of the tangential vector is modified by the definition of the FLI (Froeschlé & Lega 2000). Finally, Wu et al. (2006) developed the FLI of two nearby trajectories,

$$\text{FLI}(t) = \log_{10} \frac{d(t)}{d(0)}. \tag{38}$$

---

<sup>5</sup> The global symplectic integrators in the work of Skokos & Gerlach (2010) or Li & Wu (2011) mean that both the equations of motion and their variational equations of Hamiltonian systems simultaneously use symplectic integrations.

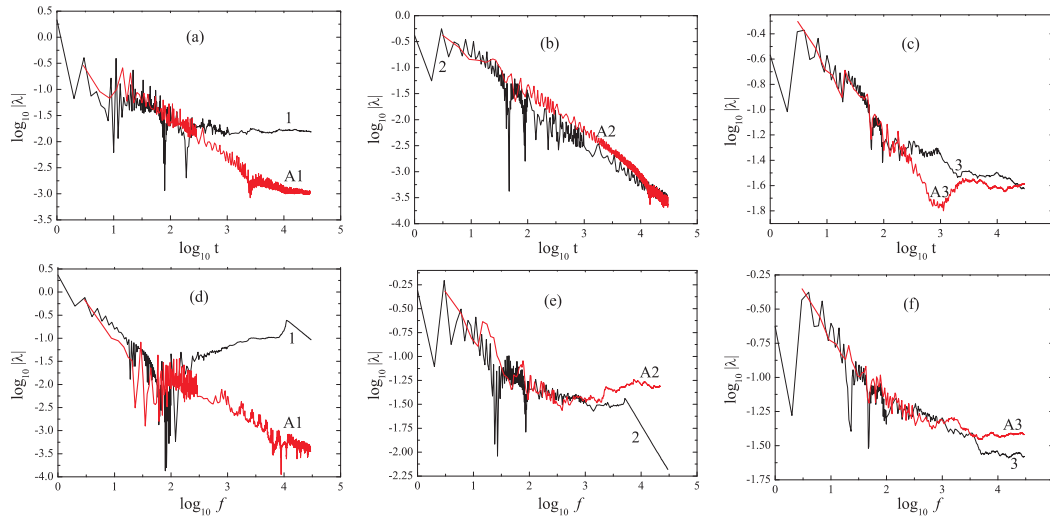


**Fig. 5** Lyapunov exponents for all the tested cases in Figs. 1 and 4(a). Note that  $e_P = 0$  in panels (a)–(c) and  $e_P = 0.01$  in panels (d)–(f). It is worth stressing that the Lyapunov exponents in the two cases of panels (a) and (d) are spurious for the nonadaptive time step methods, but they are true for the adaptive ones.

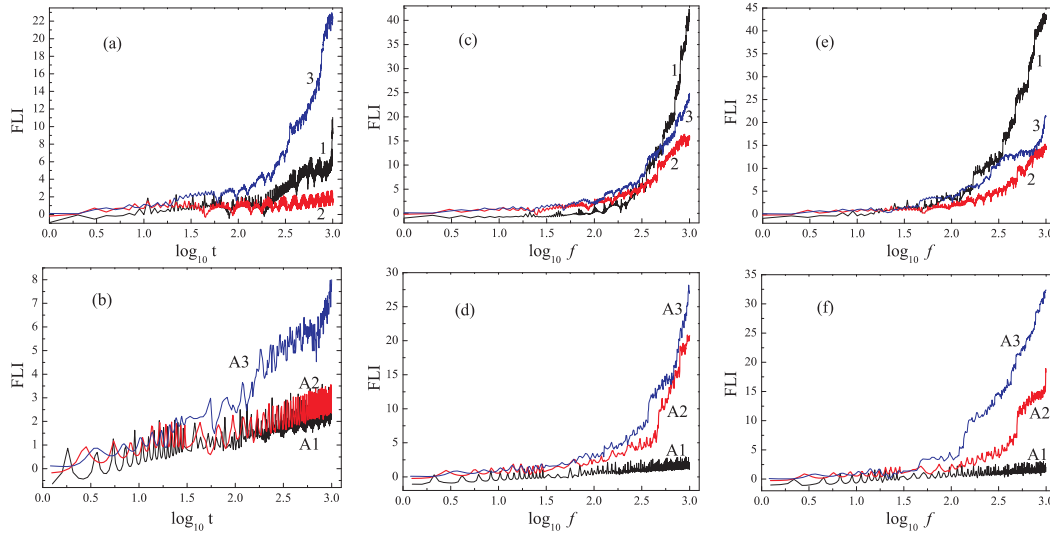


**Fig. 6** Fast Lyapunov indicators corresponding to the various cases of Fig. 5 and Fig. 4(b). Note that  $e_P = 0$  in panels (a) and (b),  $e_P = 0.01$  in panels (c) and (d), and  $e_P = 0.015$  in panels (e) and (f).

Here, two points are worth emphasizing. First, as a good choice, the starting separation  $d(0) = 10^{-9}$  is from a lot of numerical experience, and is also based on the suggestion of Wu et al. (2006). Second, the chaotic boundary will cause saturation when  $d(0) = 1$ . In this case, numerical integration no longer continues. It can be avoided through renormalization that has to be used once  $d(t) = 1$ . If the sequential number of a renormalization is  $k$ , then the indicator is computed in terms of the

following form

$$\text{FLI} = -(k + 1) \log_{10} d(0) + \log_{10} d(t). \quad (39)$$

See the article by Wu et al. (2006) or Huang et al. (2014) for more details.

If the indicator of a bounded orbit grows exponentially with time, the orbit is chaotic, but regular if the indicator increases algebraically. In light of this criterion, orbit 1 in each case of Figure 6(a), (c) and (e) seems chaotic. It should not be correct because the nonadaptive time step method gives such poor numerical accuracy and stability to the high-eccentricity orbit. When the adaptive time step method is implemented, the numerical accuracy turns out to be high enough and the numerical stability becomes better. Therefore, the spurious rapid growth of the FLI of orbit 1 can be drastically suppressed and the variation of the FLI of the orbit is typically similar to that of a regular orbit, as shown in Figure 6(b), (d) and (f). Moreover, the regularity of orbit 2 with  $e_P = 0$  and the chaoticity of orbit 2 with  $e_P = 0.01$  or  $e_P = 0.015$  are clearly depicted in these panels. In addition, orbit 3 is shown to be chaotic in the various tested cases, and the chaos of orbit 3 is stronger than that of orbit 2 in Figure 6(d) and (f). In short, Figure 6 as well as Figure 5 supports the results of Figures 3(a) and 4.

Clearly, the FLI is indeed a faster method to separate chaotic orbits from regular ones than the Lyapunov exponent. Because of this, it has been widely used in applications. For instance, it was applied to investigate capture and escape in the elliptic restricted three-body problem (Astakhov & Farrelly 2004), the chaotic dynamics in a superposed Weyl spacetime (Wu & Zhang 2006) and chaos in post-Newtonian problems of spinning compact binaries (Wu & Xie 2008; Zhong et al. 2010; Mei et al. 2013a).

#### 4 SUMMARY

The time-transformed method of Mikkola & Aarseth (2002) is refined as follows. In the extended phase space of a time-dependent Hamiltonian  $H$  with two integrable pieces, the original time  $t$  and the first new auxiliary time variable  $\tau$  are referred to as two additional coordinates, and their corresponding canonical conjugate momenta,  $-H$  and  $W$ , should also be included. Note that  $W$  is only one formal expression of the time step function, and  $g$  as a function of  $\tau$  is another approximately equivalent formal expression. Thus, Equation (19) as the canonical equations of the new time-transformed Hamiltonian  $\Gamma$  (20) with three integrable separable parts is obtained even if the part  $H_C$  or the function  $g$  does not contain explicit dependence on  $\tau$ . When an explicit symplectic integrator is applied to solve the new Hamiltonian in the second new auxiliary time variable  $s$ , it is called an adaptive time step method.

Taking the elliptic restricted three-body problem as an example of time-dependent Hamiltonian systems, we evaluate the numerical performance of our new method. It is shown in various tested cases including different orbital eccentricities of the primary bodies and the third body that the adaptive time step method compared with the nonadaptive one greatly improves the numerical accuracy by several orders of magnitude in addition to enhancing the numerical stability. In particular, it can eliminate the overestimation of Lyapunov exponents and control the spurious rapid growth of FLIs. That is to say, the reliability of Lyapunov exponents and FLIs can be guaranteed when the new adaptive time step method with sufficiently higher accuracy is used.

The present adaptive time step method is well suited not only for conservative Hamiltonian systems involving circular restricted three-body problems and  $N$ -body problems in solar system dynamics, but also nonconservative Hamiltonian systems, such as elliptic restricted three-body problems, a circular restricted three-body problem with orbital decay (Huang & Wu 2014b), post-Newtonian Hamiltonian formulations of spinning compact stars with dissipative terms (Galaviz 2011; Galaviz & Brügmann 2011) and a time-dependent barred galaxy model (Miyamoto & Nagai 1975). The separable forms of the Hamiltonian for these systems are permitted to have more choices. Additionally, a suitable choice of the time step function depends on the problem considered. In general, the time step function is associated with the potential of the problem.

**Acknowledgements** The authors are very grateful to two anonymous referees who read this manuscript in detail and gave many good suggestions that improved the presentation. This research is supported by the National Natural Science Foundation of China (Grant Nos. 11173012 and 11178002).

## References

- Astakhov, S. A., & Farrelly, D. 2004, *MNRAS*, 354, 971  
Duncan, M. J., Levison, H. F., & Lee, M. H. 1998, *AJ*, 116, 2067  
Emel'Yanenko, V. V. 2007, *Celestial Mechanics and Dynamical Astronomy*, 98, 191  
Forest, E., & Ruth, R. D. 1990, *Physica D Nonlinear Phenomena*, 43, 105  
Froeschlé, C., & Lega, E. 2000, *Celestial Mechanics and Dynamical Astronomy*, 78, 167  
Froeschlé, C., Lega, E., & Gonczi, R. 1997, *Celestial Mechanics and Dynamical Astronomy*, 67, 41  
Galaviz, P. 2011, *Phys. Rev. D*, 84, 104038  
Galaviz, P., & Brüggemann, B. 2011, *Phys. Rev. D*, 83, 084013  
Hairer, E., & Söderlind, G. 2005, *SIAM Journal on Scientific Computing*, 26, 1838  
Huang, G., & Wu, X. 2014a, *Phys. Rev. D*, 89, 124034  
Huang, G., & Wu, X. 2014b, *General Relativity and Gravitation*, 46, 1798  
Huang, G., Ni, X., & Wu X. 2014, *European Physical Journal C*, 74, 3012  
Kustaanheimo, P. E., & Stiefel, E. 1965, *Journal für die reine und angewandte Mathematik*, 218, 204  
Li, R., & Wu, X. 2011, *European Physical Journal Plus*, 126, 73  
Mei, L., Ju, M., Wu, X., & Liu, S. 2013a, *MNRAS*, 435, 2246  
Mei, L., Wu, X., & Liu, F. 2013b, *European Physical Journal C*, 73, 2413  
Mikkola, S. 1997, *Celestial Mechanics and Dynamical Astronomy*, 67, 145  
Mikkola, S., & Aarseth, S. 2002, *Celestial Mechanics and Dynamical Astronomy*, 84, 343  
Mikkola, S., & Tanikawa, K. 1999, *Celestial Mechanics and Dynamical Astronomy*, 74, 287  
Mikkola, S., & Tanikawa, K. 2013, *New Astron.*, 20, 38  
Miyamoto, M., & Nagai, R. 1975, *PASJ*, 27, 533  
Pelupessy, F. I., Jänes, J., & Portegies Zwart, S. 2012, *New Astron.*, 17, 711  
Preto, M., & Saha, P. 2009, *ApJ*, 703, 1743  
Preto, M., & Tremaine, S. 1999, *AJ*, 118, 2532  
Saha, P., & Tremaine, S. 1994, *AJ*, 108, 1962  
Seyrich, J., & Lukes-Gerakopoulos, G. 2012, *Phys. Rev. D*, 86, 124013  
Skokos, C., & Gerlach, E. 2010, *Phys. Rev. E*, 82, 036704  
Szebehely, V. 1967, *Theory of Orbits. The Restricted Problem of Three Bodies* (New York: Academic Press)  
Tancredi, G., Sánchez, A., & Roig, F. 2001, *AJ*, 121, 1171  
Wisdom, J., & Holman, M. 1991, *AJ*, 102, 1528  
Wu, X., & Huang, T.-Y. 2003, *Physics Letters A*, 313, 77  
Wu, X., Huang, T.-Y., & Zhang, H. 2006, *Phys. Rev. D*, 74, 083001  
Wu, X., & Xie, Y. 2008, *Phys. Rev. D*, 77, 103012  
Wu, X., & Zhang, H. 2006, *ApJ*, 652, 1466  
Yoshida, H. 1990, *Physics Letters A*, 150, 262  
Zhong, S.-Y., Wu, X., Liu, S.-Q., & Deng, X.-F. 2010, *Phys. Rev. D*, 82, 124040